JOURNAL OF THE KOREAN ASTRONOMICAL SOCIETY
41: 49 ~ 58, 2008 June

EFFECTS OF COLLISIONAL DE-EXCITATION ON THE RESONANCE DOUBLET FLUX RATIOS IN SYMBIOTIC STARS AND PLANETARY NEBULAE

EUN-HA KANG AND HEE-WON LEE
Department of Astronomy and Space Science, Astrophysical Research Center for the Structure and Evolution of the Cosmos, Sejong University, Seoul, 143-747, Korea
E-mail: enkang@sejong.ac.kr & hwlee@sejong.ac.kr
(Received May 19, 2008; Accepted June 19, 2008)

ABSTRACT

Resonance doublets including O VI 1032, 1038, NV 1239, 1243 and C IV 1548, 1551 constitute prominent emission lines in symbiotic stars and planetary nebulae. Spectroscopic studies of symbiotic stars and planetary nebulae from UV space telescopes show various line ratios of these doublets deviating from the theoretical ratio of 2:1. Using a Monte Carlo technique, we investigate the collisional de-excitation effect in these emission nebulae. We consider an emission nebula around the hot component of a symbiotic star characterized by the collisional de-excitation probability $p_{coll} \sim 10^{-3} - 10^{-4}$ per each resonance scattering, and the line center optical depths for major resonance doublets in the range $\tau_0 \sim 10^2 - 10^5$. We find that various line ratios are obtained when the product $p_{coll}\tau_0$ is of order unity. Our Monte Carlo calculations show that the flux ratio can be approximately fitted by a linear function of $\log \tau_0$ when $\tau_0 p_{coll} \sim 1$. It is briefly discussed that this corresponds to the range relevant to the emission nebulae of symbiotic stars.

Key words : line:formation – radiative transfer – binary:symbiotic – scattering – ultraviolet:ISM

I. INTRODUCTION

Symbiotic stars, believed to be wide binary systems consisting of a mass losing giant and a hot white dwarf, are known to exhibit prominent emission lines in the UV and optical regions. (e.g. Kenyon 1986, Mürset et al. 1991). In particular, resonance doublets including O VI 1032, 1038, N V 1239, 1243, and C IV 1548, 1551 are dominant coolants for the emission nebula surrounding the hot white dwarf component in a symbiotic star (Osterbrock 1989). They are also known to be strong in many planetary nebulae and broad emission line region in active galactic nuclei (e.g. Laor et al 1995).

These doublets arise from transitions between $S_{1/2}$ and $P_{1/2,3/2}$ states. Since $S_{1/2} - P_{3/2}$ transitions are characterized by a twice larger statistical weight than those for $S_{1/2} - P_{1/2}$, the short wavelength component is expected to be twice stronger than the long wavelength component. Therefore, this theoretical line ratio is observed from optically thin plasmas (e.g. Stenflo 1980).

However, Feibelman (1983) examined the profiles and intensity ratio of the resonance doublet C IVλ 1548, 1551 in a dozen planetary nebulae using *the International Ultraviolet Explorer* (IUE) data to find a diversity of line flux ratios ranging from 1:1 to 2:1. In a similar way, Mikolajewska, Friedjung & Quiroga (2006) reported the various flux ratios of resonance doublets in the symbiotic star CI Cyg ranging from 1.9 for N V 1239, 1243 to 1.33 for C IV 1548, 1551.

Kafatos, Michalitsianos & Fahey (1985) noted that in the symbiotic star RX Puppis the C IV 1548 component is stronger than its longer counterpart C IV 1551. This anomalous line flux ratio was attributed to the fast stellar wind driven by the central star of the planetary nebula. A similar phenomenon was reported for the symbiotic star R Aquarii by Michalitsianos et al. (1988). Schmid et al. (1999) analyzed spectroscopic data of a few symbiotic stars obtained with *the Orbiting and Retrievable Far and Extreme Ultraviolet Spectrometer* (ORFEUS) and reported that O VI 1038 is much weaker than O VI 1032 in the symbiotic stars V 1016 Cygni and Z And, which is proposed to be due to selective absorption by molecular hydrogen near 1038 Å. Except for these kinds of anomalous examples, it seems that no physical explanations have been proposed for the phenomena of various line flux ratios exhibited in resonance doublets (e.g. Schmid et al. 1999, Yoo, Lee & Ahn 2002).

According to Adams (1972), resonance line photons escape from an optically thick medium by a process called '*single longest excursion*'. In this process, line photons suffer a large number of resonance scatterings near the site of the generation before they acquire a huge frequency shift to make a long excursion and

Corresponding Author: H.-W. Lee

emerge from the scattering medium. The typical number of scatterings before escape is approximately equal to the line center optical depth τ_0, from which we expect that the line photons associated with the transition $S_{1/2} - P_{3/2}$ will be scattered almost twice as many times as those for $S_{1/2} - P_{1/2}$.

It is expected that resonance line photons may be collisionally de-excited, which results from inelastic collision with free electrons in the scattering medium. In particular, Bonilha (1979) studied intensively the effect of collisional de-excitation on the scattering numbers and emergent flux (see also Frisch 1980). We revisit this problem in the particular context on the line flux ratios of resonance doublets. The collisional de-excitation may affect the emergent line flux more severely for line photons with $S_{1/2} - P_{3/2}$ than those with $S_{1/2} - P_{1/2}$, because the former will stay in the medium longer than the latter with the enhanced chance of being destroyed by collisional de-excitation. If this effect of collisional de-excitation is not exactly twice larger for line photons with $S_{1/2} - P_{1/2}$, then we may expect deviations of the line flux ratios from the ratio 2:1.

In this paper, we investigate the effect of collisional de-excitation on the flux ratios in an optically thick emission region by a Monte Carlo technique without the consideration of the damping wing. In the next section, we describe our Monte Carlo calculations for the transfer of resonance line photons. In Section 3, the numerical results are presented. We give a brief discussion on the observations that are relevant to our Monte Carlo calculations.

II. MODELS AND CALCULATION

(a) Physical Conditions of Emission Nebulae in Symbiotic Stars

In this subsection, we describe the physical conditions that are believed to be pertinent to compact emission nebulae in symbiotic stars. According to Schmid et al.(1999), the observed flux of the O VI doublet for the symbiotic nova RR Tel is of order $F_{OVI} \sim 10^{-10}$ erg cm^{-2} s^{-1}. If this source is located 1 kpc away from us, this observed line flux is directly translated into the line luminosity $L_{OVI} \sim 10^{34}$ erg s^{-1}.

The emission nebula of a symbiotic star may not be described by a single value of electron density. However, for simplicity, we adopt a simple model of an emission nebula characterized by a single electron number density

$$n_e \sim 10^{10} \text{ cm}^{-3}, \quad (1)$$

which permits the formation of semi-forbidden line C III]1909 (e.g. Mikolajewska et al. 2006).

According to Osterbrock (1989), the collision time t_C of an ion with a free electron is given by

$$t_C \sim \left[n_e \frac{8.629 \times 10^{-6}}{T^{1/2}} \frac{\Omega(1,2)}{\omega_2} \right]^{-1}$$

$$\sim 1.4 \times 10^{-3} \left(\frac{10^{10} \text{ cm}^{-3}}{n_e} \right) \left(\frac{T}{10^4 \text{ K}} \right)^{1/2} \text{s} \quad (2)$$

where T is the electron temperature of the emission nebula.

Here, ω_2 is the statistical weight of the excited state for the O VI doublet transition and $\Omega(1,2)$ is the collision strength, for which we take the value $\Omega(1,2) = 5.00$ given by Osterbrock (1989). Considering that a typical time scale for a radiative de-excitation for a permitted transition is of order $t_R \sim 10^{-8} - 10^{-9}$ s, this implies that the probability p_{coll} for collisional de-excitation per scattering is given by the ratio of the collisional and radiative time scales

$$p_{coll} \equiv \frac{t_R}{t_C}. \quad (3)$$

We note that $p_{coll} \sim 10^{-5} - 10^{-6}$ for an emission plasma with $n_e \sim 10^{10}$ cm^{-3}.

Many studies on the radiative transfer of resonantly scattered line photons show that the number of scatterings before escape is approximately given by the line center optical depth τ_0 of the scattering medium (e.g. Adams 1972, Harrington 1973, Neufeld 1990, Ahn, Lee & Lee 2001). If the emission plasma is characterized by a line center optical depth $\tau_0 \sim 10^5$, then we expect that the effect of collisional de-excitation will be quite significant.

By adopting an electron density given by Eq. (1), the collisional excitation rate $< \sigma v >= 10^{-7}$ cm^3 s^{-1}. Also adopting a typical abundance of O VI, the O VI ion number density $n_{OVI} \sim 10^{-4} n_e$. Here, we also assume that the dominant ionization stage for oxygen is O VI in this emission plasma (e.g. Osterbrock 1989). Combining these quantities, we estimate the O VI line luminosity

$$L_{OVI} \sim n_e n_{OVI} < \sigma v > S^3$$

$$\sim 10^{34} \left(\frac{n_e}{10^{10} \text{ cm}^{-3}} \right)^2 \left(\frac{S}{10^{12} \text{ cm}} \right)^3 \text{erg s}^{-1}. \quad (4)$$

Here, S is the linear dimension of the emission region. If we adopt a typical distance to a symbiotic star $d \sim 1$ kpc, we infer that the emission region has a volume of order $V \sim 10^{36}$ cm^3, leading to the physical dimension of order $S \sim 10^{12}$ cm.

Considering a typical line center cross section $\sigma_{\nu_0} \sim 10^{-13}$ cm^2 for a resonance line photon in a medium with temperature $T \sim 10^4$ K (e.g. Rybicki & Lightman 1979), we note that this emission region with $n_{OVI} \sim 10^6$ cm^{-3} and size $S \sim 10^{12}$ cm is characterized by line center optical depth $\tau_0 \sim 10^5$. The emission measure of order 10^{58} cm^{-3} for CI Cyg proposed by Mikolajewska et al. (2006) is consistent with our estimate.

(b) Monte Carlo Procedure

In this work, for the sake of simplicity, two types of scattering geometry are considered, one being a slab

with a finite thickness and the other a sphere with a finite radius. All the scattering regions are assumed to be uniform, so that the physical distance is exactly proportional to line center optical depth τ_0, with which we describe the physical dimension of the scattering regions. We measure the thickness of a slab by line center optical depth τ_0 from the midplane to the surface along the normal direction. In the case of a sphere, the optical depth is measured from the center of the sphere.

The scattering cross section σ_ν of electromagnetic radiation with an atomic electron near resonance is approximated by a Lorentzian with the property

$$\int \sigma_\nu \, d\nu = \frac{\pi e^2}{m_e c} f_{osc}, \tag{5}$$

where f_{osc} is the oscillator strength, m_e and e are the electron mass and charge, respectively (e.g. Rybicki & Lightman 1979). If we ignore the radiation damping, the scattering cross section can be simply written using the Dirac delta function

$$\sigma_\nu = \frac{\pi e^2}{m_e c} f_{osc} \delta(\nu - \nu_0), \tag{6}$$

due to the smallness of the Lorentzian width compared to the thermal width.

Because the scattering region is governed by a Maxwell-Boltzmann distribution with a temperature T, the scattering optical depth τ_0 for a photon at line center frequency ν_0 is given by

$$\tau_0 = N_i \frac{\pi e^2}{m_e c} f_{osc} \frac{1}{\sqrt{\pi} \Delta\nu_D}, \tag{7}$$

instead of the Voigt function in the presence of radiation damping. Here, N_i is the scattering ion column density and $\Delta\nu_D = \nu_0 v_{th}/c = \nu_0 \sqrt{\frac{2kT}{m_i}}/c$ is the Doppler frequency width with m_i and v_{th} being the ion mass and the thermal velocity, respectively.

The damping wing part associated with the natural broadening should be important in an optically thick medium with $\tau_0 > a$, where a is the ratio of the natural broadening width to that of the Doppler broadening. In a medium with a temperature $T \sim 10^4$ K, the thermal motion is of order 10 km s^{-1} and the natural width is of order $10^{-8}c$, leading to $\tau_W \sim 10^4$ where the damping wing part starts to become significant.

In emission nebulae of symbiotic stars, a typical line center optical depth $\tau_0 \sim 10^5$ exceeding τ_W, and hence the effect of damping term should be considered with full care in order to obtain an accurate description of line radiative transfer. A full discussion of the observed flux ratios in symbiotic stars requires a numerical study with the scattering cross section given by a Voigt function. We defer this study as a future work and concentrate on the flux ratio that may change as a function of scattering numbers in moderately thick media.

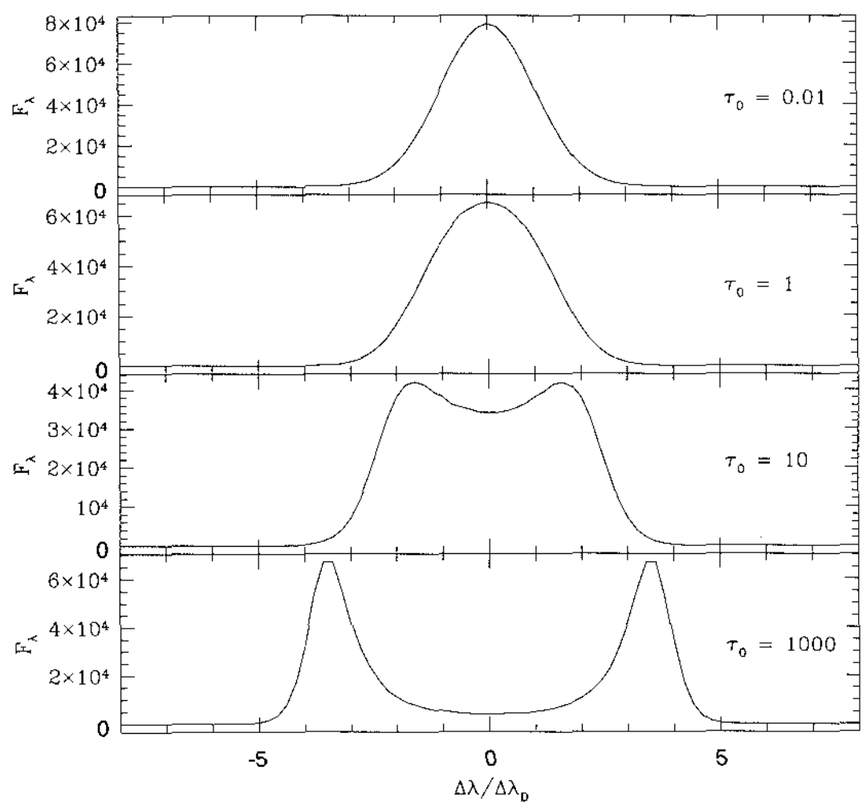

Fig. 1.— Typical line profiles for a range of line center optical depths of finite slabs. The horizontal axis shows the wavelength deviation from line center ($\Delta\lambda = \lambda - \lambda_0$) in units of the Doppler width $\Delta\lambda_D = \lambda_0 v_{th}/c$. Because the transfer of resonance line photons is a diffusion process both in real space and frequency space, the emergent profiles exhibit double peak profiles for large optical depths.

In a stationary scattering medium, we introduce a weighting factor ρ for each photon generated in the medium, which is initially assigned to be unity. To each photon generated at the initial position $\mathbf{R}_i$, we assign the initial unit wavevector $\hat{\mathbf{k}}_i$ and the initial frequency parameter $x_i = (\nu_i - \nu_0)/\Delta\nu_D$ using the Gaussian random deviate "*gasdev*" prepared by Vetterling et al. (1985). A uniform random deviate r in the interval $(0, 1)$ is generated to yield the physical path length of this line photon to the next scattering site, which is given by

$$l = -l_0 e^{x_i^2} \ln(1 - r). \tag{8}$$

Here, l_0 is the physical length corresponding to unit line center optical depth $\tau_0 = 1$.

If the next scattering position given by $\mathbf{R}_f = \mathbf{R}_i + l\hat{\mathbf{k}}_i$ is inside the scattering region, we assign a new unit wavevector $\hat{\mathbf{k}}_f$ for the scattered photon. Here, $\hat{\mathbf{k}}_f$ is chosen to be isotropic irrespective of $\hat{\mathbf{k}}_i$. This is physically sound for line photons corresponding to $S_{1/2} - P_{1/2}$ (e.g. Stenflo 1980). However, the direction of $\hat{\mathbf{k}}_f$ depends on $\hat{\mathbf{k}}_i$ in the case $S_{1/2} - P_{3/2}$, but in an optically thick medium, the resultant flux is almost indistinguishable with that obtained under the assumption of isotropy in $\hat{\mathbf{k}}_f$.

The new frequency x_f of the scattered photon is assigned under the coherency of scattering in the rest frame of the scattering atom (e.g. Hummer 1962). In

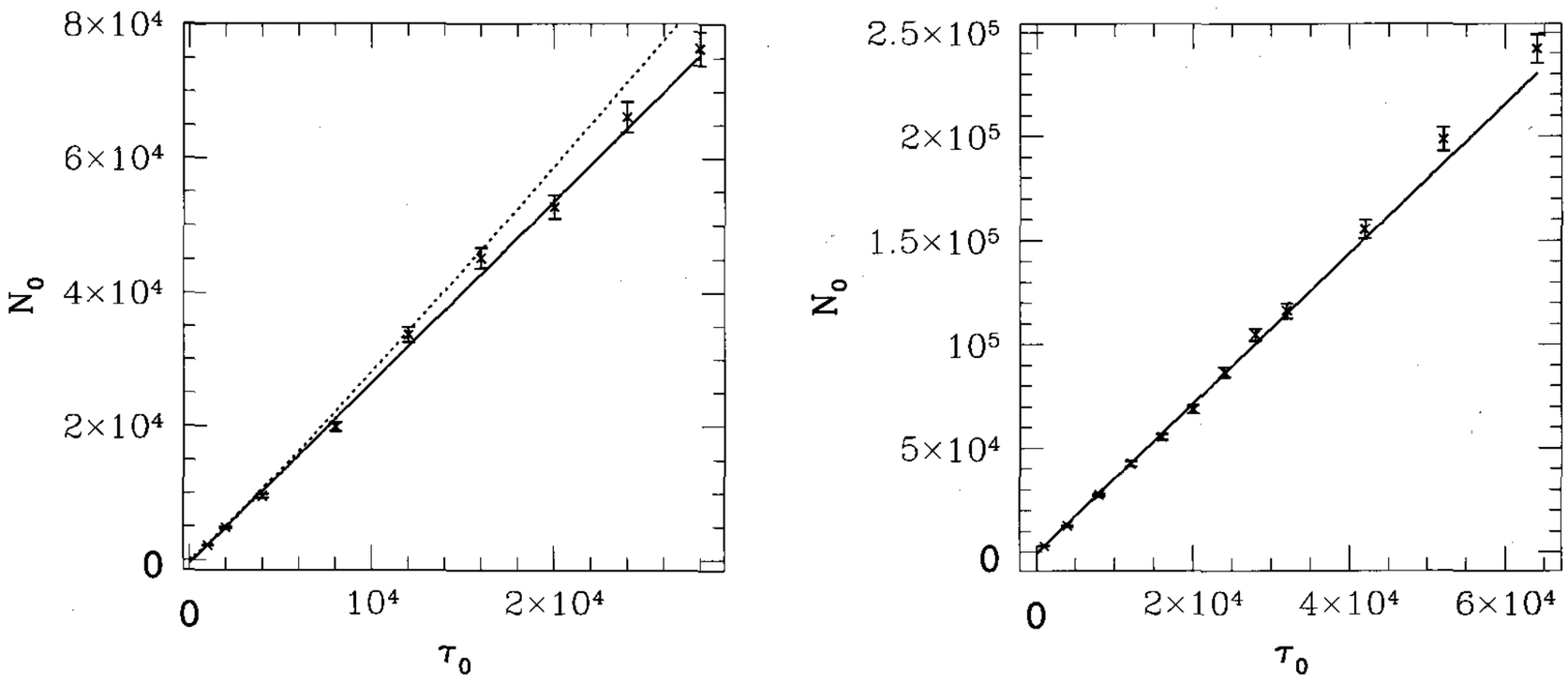

Fig. 2.— Mean number of resonance scatterings before escape from a finite slab. The crosses show our Monte Carlo results, where the vertical error bars are the standard deviations. We also fit the data linearly by minimizing the chi square, which is shown by solid lines. The dotted line in the left panel shows the analytical result $N_0 = \tau_0[\ln \tau_0/2\sqrt{\pi}]^{1/2}$ proposed by Avrett & Hummer (1965).

our Monte Carlo code, this is accomplished by generating a Gaussian random deviate x_g and setting

$$x_f = x_i(\hat{\mathbf{k}}_i \cdot \hat{\mathbf{k}}_f) + x_g[1 - (\hat{\mathbf{k}}_i \cdot \hat{\mathbf{k}}_f)^2]^{1/2}. \quad (9)$$

As we follow each photon from its position of generation until escape, the weighting factor ρ is reduced by a factor $1-p_{coll}$ per scattering, considering that the fraction p_{coll} is removed from the line flux via collisional de-excitation. This procedure ends when the location of the next scattering is outside the scattering region, in which case the line photon escapes and reaches the observer with the relative flux ρ. In this work, we do not consider the angular distribution of emergent photons and add all the flux weights ρ associated with escaping photons.

Collisional de-excitation becomes very important for line photons that may suffer $\sim N$ scatterings, where $N \sim p_{coll}^{-1}$. Despite the fact that the relevant values of $p_{coll} = 10^{-5}$ and hence $\tau_0 \sim 10^5$, we consider slabs and spheres with τ_0 slightly less than 10^5. Instead, we consider slightly larger values of p_{coll}, from which we scale our results to relevant emission nebulae.

III. RESULTS

(a) Line Profiles and Mean Scattering Numbers

In this subsection, we provide our results on the scattering numbers before escape and line profiles of emergent line photons. This subject has been studied by many researchers and we present this result as a check of our code.

In Fig. 1, we show typical line profiles for a range of line center optical depths of finite slabs assuming no collisional de-excitation. In the figure, τ_0 denotes the line center optical depth from the midplane to the surface. The horizontal axis represents the wavelength shift $\Delta\lambda = \lambda - \lambda_0$ in units of the Doppler width $\Delta\lambda_D = \lambda_0 v_{th}/c$. In the case $\tau_0 = 0.01$ where the medium is very optically thin, the resultant profile is almost the same as the initial source profile, which is a simple Gaussian function. As τ_0 increases, escape is achieved through diffusion in the frequency space, leading to profile broadening both redward and blueward. As a result, for optically thick media, symmetric profiles with a double peak structure are obtained (e.g. Neufeld 1990, Ahn, Lee & Lee 2001). The peak locations for $\tau_0 = 10$ and $\tau_0 = 10^3$ are $\Delta\lambda/\Delta\lambda_D = \pm 1.5$ and ± 3.5, respectively.

In Fig. 2, we show the mean number of resonance scatterings before escape from a slab with finite thickness. The horizontal axis shows the line center optical depth τ_0 along the normal direction to the slab plane, and the vertical axis represents the mean number of scatterings before escape. In this calculation, we also assume that no collisional de-excitation operates in the scattering region, in order to concentrate on the scattering number of photons in a given scattering region.

In the left panel of Fig. 2, we show our results from finite slabs, where the initial photons are generated in the entire region uniformly. Our Monte Carlo results are shown by dots, and the solid line shows our linear fit to the numerical data. For $\tau_0 = 1.6 \times 10^5$, we have the mean number of scatterings $N_{scat} = 4.7 \times 10^5$. Because

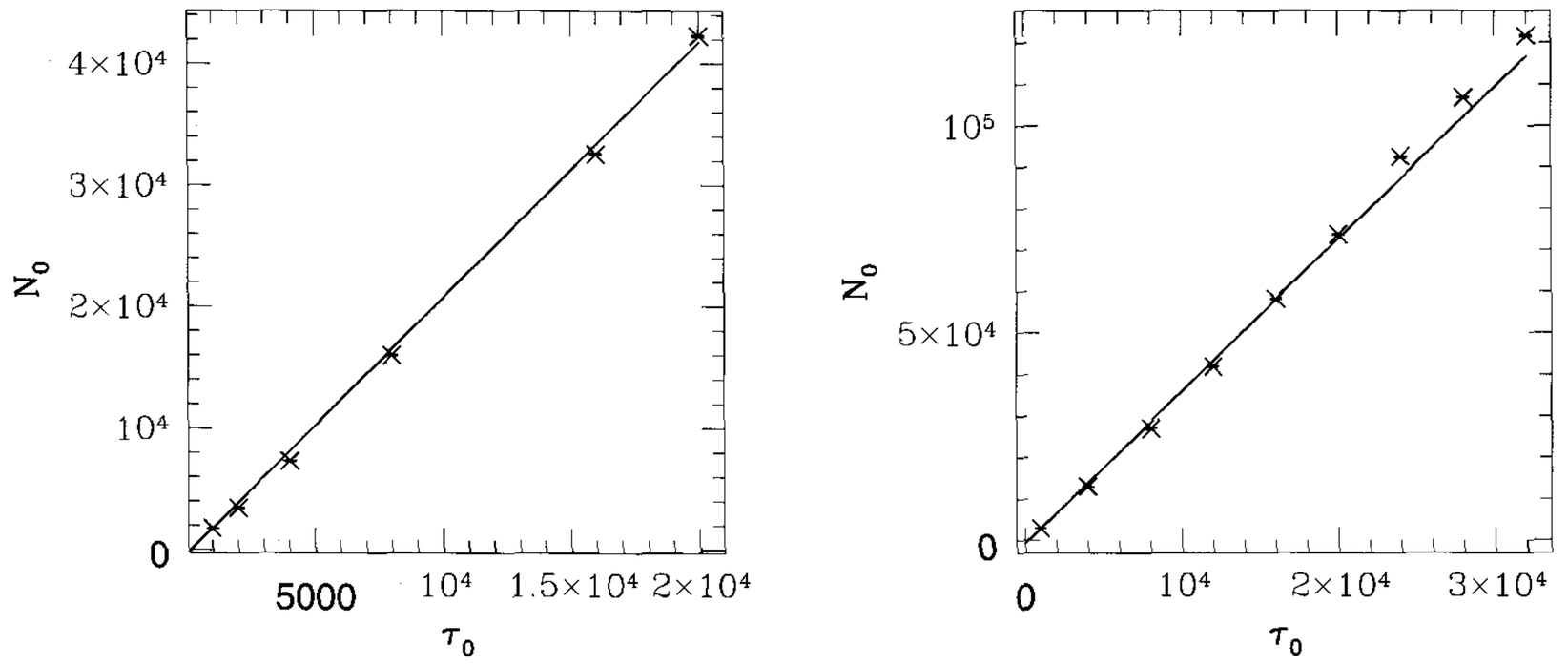

Fig. 3.— Mean number of resonance scatterings before escape from a finite sphere. The crosses show our Monte Carlo results, where the vertical error bars are the standard deviations. We also fit the data linearly by minimizing the chi square.

our numerical results are excellently fitted by a straight line, the least chi square method is applied to obtain

$$N_{scat}(\tau_0) \simeq 2.7\tau_0. \tag{10}$$

This result was also obtained by Adams (1972) with the same linear relation.

Another fit to our data for finite slabs is shown by a dotted line with the analytical result

$$N_0 = \tau_0[\ln(\tau_0/2\sqrt{\pi})]^{1/2}, \tag{11}$$

which was obtained by Avrett & Hummer (1965) using the asymptotic forms of the kernel function of the line radiative transfer equation (see also Hummer & Rybicki 1971). When $\tau_0 < 10^3$ the agreement between the Monte Carlo data and Eq. (11) is excellent, and however a slight deviation is seen for $\tau_0 \sim 10^4$. Bonilha (1979) proposed that the mean number of resonance scatterings is given by

$$N_0 \simeq [1.6 + 1.5/(a\tau_0)] \times \tau_0 \tag{12}$$

when the damping wing part is also considered. Here, a is the damping coefficient divided by the Doppler width. Therefore, this approximate formula yields slopes that are slightly larger or smaller than our value 2.7 for different choices of a.

In the right panel, we also show our results for the same slabs, where the initial photons are generated only at the midplane. The linear fit is also excellent and the results are qualitatively similar to those shown in the left panel except for the proportionality constant. For $\tau_0 = 64000$, the mean number of scatterings is 242089, from which we obtain

$$N_{scat,midplane} \simeq 3.6\tau_0, \tag{13}$$

for midplane sources. This is quite significantly steeper than the relation shown in Eq. (10) for the same geometry with the source distributed in the entire region.

In Fig. 3 we consider a spherical scattering region that is characterized by the line center optical depth τ_0 from the center to the surface. The horizontal and vertical axes represent the line center optical depth from the center to the surface and the mean number of scatterings before escape, respectively, similarly as in the case of Fig. 2. The crosses show our Monte Carlo result, whereas the solid linear lines show our fit to the numerical data.

In the left panel of Fig. 3, line photons are generated uniformly inside the entire scattering region. The numerical data are well fitted by the linear relation

$$N_{scat}^{sph} \simeq 2.0\tau_0. \tag{14}$$

It is noted that the proportionality constant 2.0 is significantly smaller than the counterpart for the slab case. This large difference is attributed to the contribution from those photons initially generated near the boundary.

In the right panel of Fig. 3, we also show our results for the same spheres, where the initial photons are generated at the center. The linear fit is given by

$$N_{scat,center}^{sph} \simeq 3.6\tau_0. \tag{15}$$

It is quite interesting that the proportionality constant is almost similar to the value for a finite slab with the same thickness.

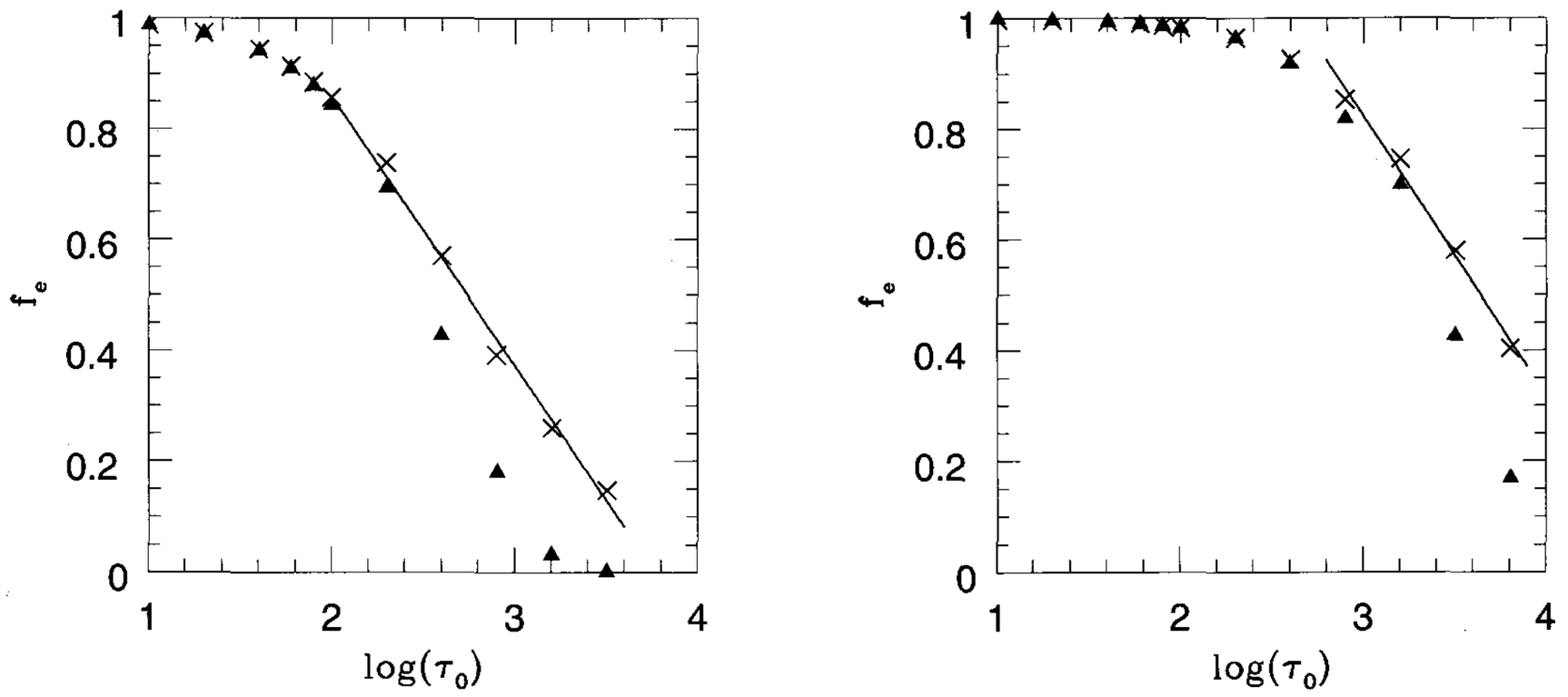

Fig. 4.— Escape fraction of resonantly scattered photons from a finite slab. The crosses show our Monte Carlo results. The data are linearly fitted by minimizing the chi square. The left panel is for $p_{coll} = 10^{-3}$, and the right panel is for $p_{coll} = 10^{-4}$, where p_{coll} is the probability of collisional de-excitation per resonance scattering.

(b) Escape Fractions and Resonance Doublet Flux Ratios

In this subsection, we consider the effect of collisional de-excitation on the escape fraction, which eventually leads to the variation of resonance doublet flux ratios. We consider a similar range of parameters for the same scattering geometry considered in the previous section with our two choices of collisional de-excitation probability $p_{coll} = 10^{-3}$ and 10^{-4} per scattering.

In Fig. 4, we show the escape fraction f_e, which is defined as the ratio of the number of emergent photons to that of created photons inside a finite slab. In the left panel, the result for $p_{coll} = 10^{-3}$ is shown and the right panel is for $p_{coll} = 10^{-4}$. The crosses are our numerical data, and the solid line is obtained from the least square method.

The filled triangles show the probability f_c given by

$$f_c = (1 - p_{coll})^{N_0}, \tag{16}$$

which would give the probability of collisional de-excitation for line photons with exactly N_0 resonance scatterings. Here, for N_0 we use the mean number of resonance scatterings in the absence of collisional de-excitation, which is obtained in the previous subsection.

Naively we may expect that the photon loss rate is given by Eq. (16) under the assumption that all the photons suffer the same number of scatterings. As seen in Fig. 4, the numerical result shows good agreement with this expectation when the scattering optical depth is not large and photon loss due to collisional de-excitation is negligible. Therefore, in an optically thin medium with line center optical depth τ_0 and mean scattering number N_0 before escape, the escape fraction is approximated by

$$f_{e,thin} \simeq 1 - N_0 p_{coll}, \tag{17}$$

in which we note that $N_0 p_{coll} \ll 1$.

However, we observe significant deviations from this simple expectation as the line center optical depth increases. The deviation is attributed to the fact that each photon suffers different scattering number and a dominant contribution is due to those photons with less scattering numbers. When the escaping fraction $f_{e,slab}$ is less than 0.8, we note that it is linearly dependent on the logarithm of line center optical depth τ_0, which is given by

$$f_{e,slab} = -0.49 \log \tau_0 + 1.85 \tag{18}$$

for $p_{coll} = 10^{-3}$. When $p_{coll} = 10^{-4}$, the linear fit is given by

$$f_{e,slab} = -0.50 \log \tau_0 + 2.34 \tag{19}$$

It is noted that the slopes of the linear fits for both cases are similar. In particular, half of line photons survive when $\log_{10} \tau_0 \simeq 2.8$ for $p_{coll} = 10^{-3}$ and $\log_{10} \tau_0 = 3.7$ for $p_{coll} = 10^{-4}$.

In Fig. 5, we show the escape fraction $f_{e,sph}$ for finite spheres with $p_{coll} = 10^{-3}$ and $p_{coll} = 10^{-4}$. We obtain qualitatively similar results, where the linear fits are given by

$$f_{e,sph} = \begin{cases} -0.48 \log \tau_0 + 1.86, & p_{coll} = 10^{-3} \\ -0.47 \log \tau_0 + 2.25, & p_{coll} = 10^{-4} \end{cases}. \tag{20}$$

Again, similar behaviors are obtained in the cases of spherical scattering geometry. A half of photon loss is seen when $p_{coll} \tau_0 \simeq 10^{-0.3}$ in both cases.

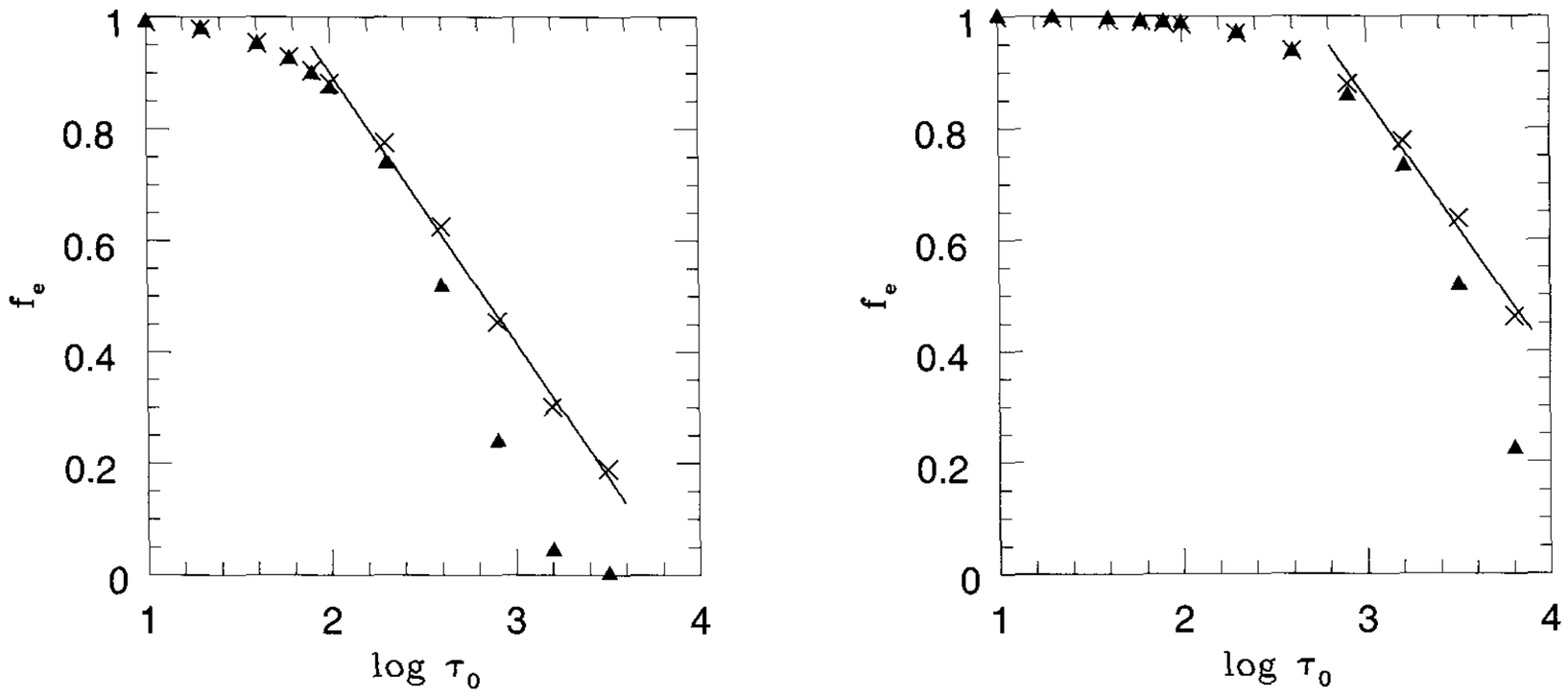

Fig. 5.— The same quantities as in Fig. 4 for finite spheres.

In Fig. 6, we show the resonance doublet flux ratios from a finite slab subject to the collisional deexcitation. Here, the flux ratio R is defined as the ratio of the emergent flux of the short wavelength component $(S_{1/2} - P_{3/2})$ to that of the long wavelength component $(S_{1/2} - P_{1/2})$. The horizontal axis is the logarithm of line center optical depth for the long wavelength component, which we denote by τ_L. The theoretically expected ratio in the absence of photon loss is 2, which is attained in the optically thin limit.

The left panel shows our Monte Carlo results for $p_{coll} = 10^{-3}$ and the right panel is for $p_{coll} = 10^{-4}$ in the range of line center optical depths $\tau_L > 0.1 p_{coll}^{-1}$, and $\tau_L > 0.05 p_{coll}^{-1}$ respectively. The flux ratio R decreases linearly with the logarithm of τ_L when $\tau_L > 0.1 p_{coll}^{-1}$. It is noticeable that the flux ratio is less than 1 for $\tau_L > 10^{3.5}, p_{coll} = 10^{-3}$, in which case less than 10 percent of $S_{1/2} - P_{3/2}$ photons may survive and escape as shown in Fig. 4.

The linear fit for $p_{coll} = 10^{-3}$ is

$$R = -0.44 \log \tau_L + 2.58. \tag{21}$$

In the case of $p_{coll} = 10^{-4}$, the linear fit is

$$R = -0.41 \log \tau_L + 2.91. \tag{22}$$

The slopes of the two linear fits are similar and therefore the linear fit for the case $p_{coll} = 10^{-4}$ almost coincides with the line that is translated from the linear fit of $p_{coll} = 10^{-3}$ by unity along the horizontal axis. In particular, the flux ratio of 1.5 is obtained for $\tau_L = 10^{2.6}$, $p_{coll} = 10^{-3}$, and $\tau_L = 10^{3.4}$, $p_{coll} = 10^{-4}$. From this, we may infer that the flux ratio of 1.5 is obtained if the emission region satisfies $p_{coll}\tau_L \sim 10^{-0.5}$.

In Fig. 7 we show the same quantities as in Fig. 6 for spherical scattering geometry. In a similar way to finite slabs, the flux ratio of 1.5 is obtained when $p_{coll}\tau_L \sim 10^{-0.5}$. The linear fits are given by

$$R = \begin{cases} -0.36 \log \tau_L + 2.43, & p_{coll} = 10^{-3} \\ -0.36 \log \tau_L + 2.79, & p_{coll} = 10^{-4} \end{cases}. \tag{23}$$

For spheres, the slopes are somewhat smaller than those obtained for finite slabs.

In an optically thin medium with $N_0 p_{coll} \ll 1$, the flux ratio is given by

$$\begin{aligned} R &= \frac{2 f_e^s}{f_e^l} \simeq \frac{2(1 - N_0 p_{coll})}{1 - N_0 p_{coll}/2} \\ &= 2 - N_0 p_{coll} \simeq 2 - A \tau_L p_{coll}, \end{aligned} \tag{24}$$

where A is a numerical factor of order unity that depends in detail on the specific scattering geometry.

We note that the flux ratios are approximately given by a linear function of $\log \tau_0$ when $\tau_0 p_{coll}$ is of order unity. Noting that $\sigma_{\nu_0} \sim 10^{-13}$ cm^2, the condition $\tau_0 p_{coll} \sim 1$ for an atomic species with abundance A_i relative to electron is met in an ionized nebula with a physical dimension S satisfying

$$S n_e^2 \sim \left(\frac{A_i}{10^{-4}} \right) 10^{32} \text{ cm}^{-5}. \tag{25}$$

As is discussed in the previous section, this is quite relevant in symbiotic stars. In addition, this condition appears to be met in the broad emission line region of a typical active galactic nuclei, for which much larger velocity scale hinders the decomposition of the doublets

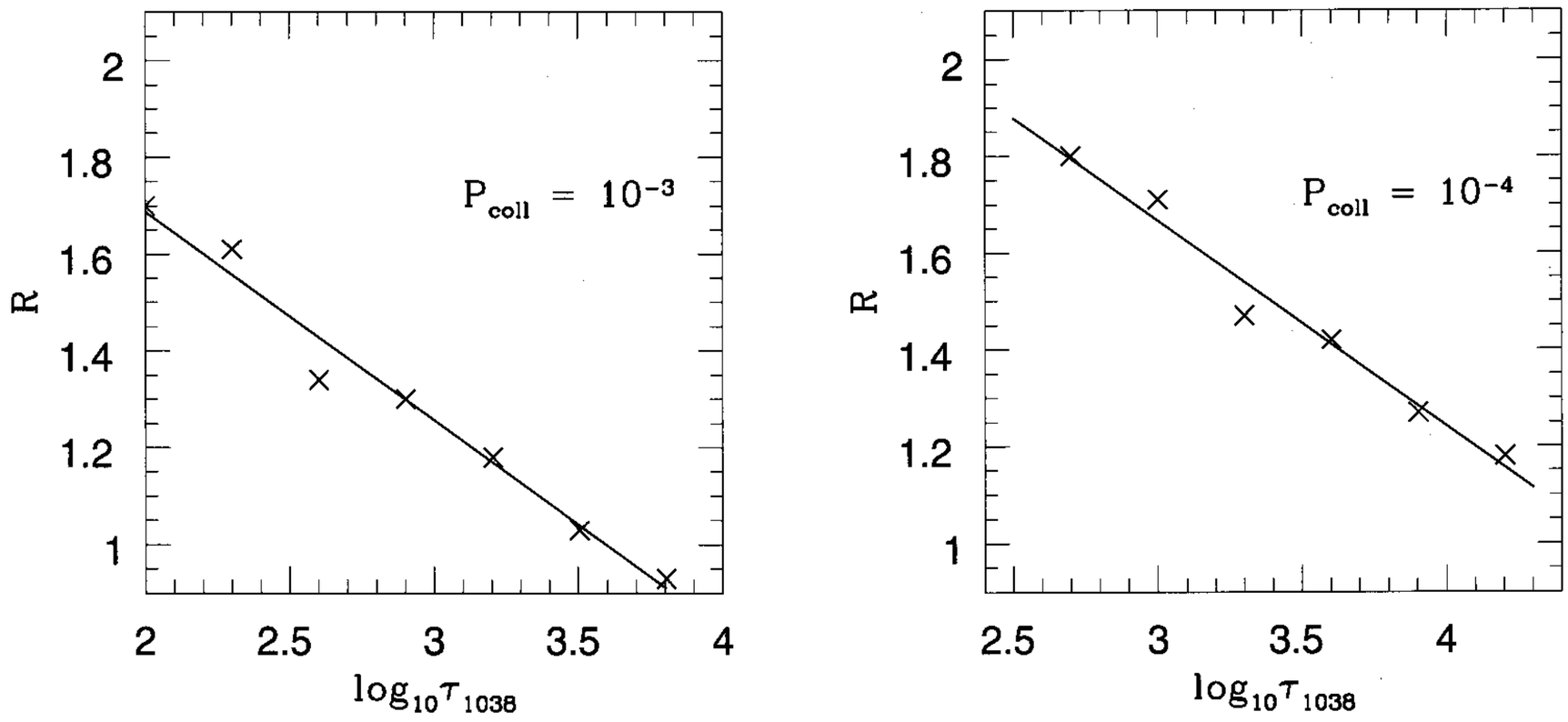

Fig. 6.— Resonance doublet flux ratios from a finite slab subject to the collisional de-excitation. The left panel is for $p_{coll} = 10^{-3}$ and the right panel is for $p_{coll} = 10^{-4}$, where p_{coll} is the probability of collisional de-excitation per resonance scattering. The crosses show our Monte Carlo results, and the data are linearly fitted by minimizing the chi square.

into each component (e.g. Osterbrock 1989, Laor et al. 1995).

In Figs. 4 through 7, it should be pointed out that the linear fits are taken with caution. Because of the narrow meaningful ranges of $f_e \leq 1$ and $R \leq 2$ and sparse data points, the linear fits have limited validity in quite a small parameter space with $\tau_0 p_{coll} \sim 10^{-1} - 10^{0}$. Globally, the linearity of f_e is incompatible with the linearity R, and hence more refined calculations are required in order to obtain more reliable functional dependence of R on τ_0 and p_{coll}.

IV. SUMMARY AND DISCUSSION

In this work, we propose that various resonance doublet flux ratios can result due to collisional de-excitation effects in a medium with a large scattering optical depth. Given p_{coll} that is defined as the ratio of the time scales associated with collisional de-excitation and radiative de-excitation, significant deviations from the theoretically expected ratio of 2 are seen when the product $p_{coll}\tau_0$ becomes of order unity. The emission nebulae in symbiotic stars may be characterized by line center optical depth $\tau_0 \sim 10^5$ for typical resonance doublets including O VI 1032, 1038, N V 1239, 1243 and C IV 1548, 1551 and the probability of collisional de-excitation per scattering $p_{coll} \sim 10^{-5}$, and hence they satisfy the condition for exhibiting various resonance doublet flux ratios. However, it should be noted that the realistic emission nebulae may not be described by a single value of τ_0 nor by a single value of p_{coll}. Instead, depending on the location, we may expect a range of these values from $\tau_0 \sim 10^4 - 10^6$ and $p_{coll} \sim 10^{-4} - 10^{-6}$.

The realistic line center optical depths of $\tau_0 \sim 10^5$ in emission nebulae of symbiotic stars are higher than those considered in this work. Furthermore, scattering in the damping wing region is also ignored, which should be important in highly thick media with $\tau_0 > 10^4$. In this study we verified that the photon destruction ratio is not directly proportional to the line center optical depth, leading to diverse flux ratios in resonance doublets. This result implies that a similar reasoning may apply to higher media. More careful approach incorporating these effects are deferred to a future work.

Another interesting example is provided from the different line profiles exhibited by Raman scattered O VI 6825 and 7088 in some symbiotic stars (Schmid 1989, Harries & Howarth 1996, Schmid et al. 1999). These scattered features originate from inelastic scattering of the resonance doublet O VI 1032, 1038 by atomic hydrogen (Schmid 1989). In a number of symbiotic stars including V1016 Cyg and RR Tel, the blue part of Raman O VI 7088 is relatively more suppressed than the corresponding part in Raman O VI 6825. This may indicate the operation of line transfer effects in locally inhomogeneous emission nebulae, which leads to various flux ratios.

This point is particularly interesting when we adopt an accretion disk emission model, in which the line center optical depth may differ locally and hence the effect of collisional de-excitation can complicate the line profiles (e.g. Mastrodemos & Morris 1998, Lee & Park 1999). Lee & Kang (2007) demonstrated that the profiles of the O VI Raman-scattered 6825 in the symbiotic novae V 1016 Cygni and HM Sagittae are consistent with the emission region in the form of an accretion flow in Keplerian motion with the physical extent of $\sim$ 1 AU. This estimate may be combined with the emission volume $V \sim 10^{36}$ cm^3 to imply that the emis-

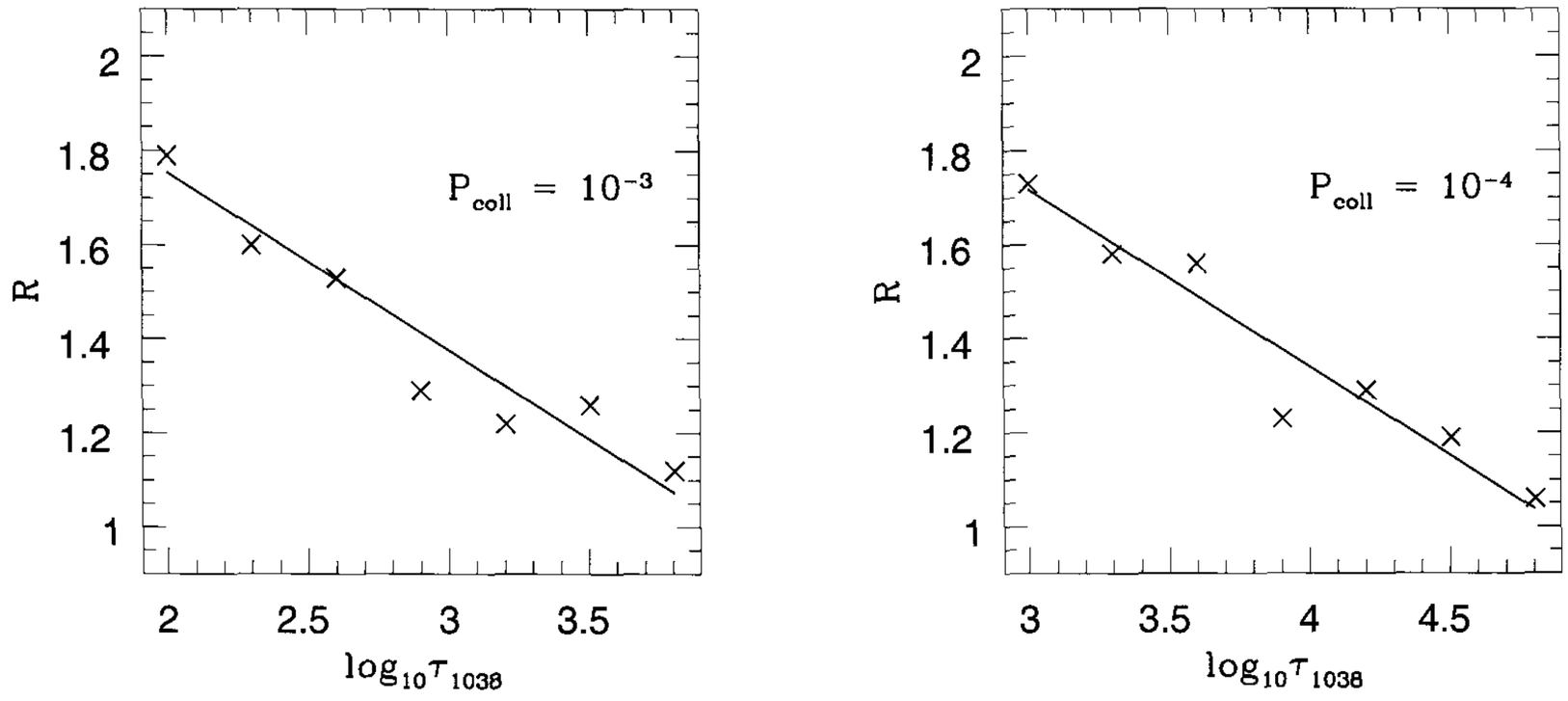

Fig. 7.— The same quantities as in Fig. 6 for finite spheres.

sion region may be geometrically quite thin.

Another consequence of this study is that various resonance doublets may exhibit different flux ratios, because of differing abundances, ionization structures and quantum numbers associated with collision and radiative interactions. This is illustrated in the IUE data of the symbiotic star CI Cyg pointed out by Mikolajewska et al. (2006). This fact may be used to provide important constraints on the detailed nebular conditions with more sophisticated theoretical considerations.

It is very well known that the scattering number before escape is greatly affected by the velocity gradient that may be present in an emission region subject to a complicated kinematics such as expansion and differential rotation. Because the line profile is also severely influenced from the kinematic structure, spectroscopic data should be analyzed with this point in mind. In particular, when the scale of the velocity difference in the emission region is much larger than the thermal width, one normally adopts the Sobolev approximation (e.g. Hummer & Rybicki 1982), which may be an appropriate approach to stellar wind of early type stars and quasar broad absorption line region. The validity of the Sobolev approximation in emission nebulae of symbiotic stars and planetary nebulae is questionable, and a careful approach is required.

ACKNOWLEDGEMENTS

We are very grateful for the careful and constructive comments by an anonymous referee. The authors gratefully acknowledge financial support from the Astrophysical Research Center for the Structure and Evolution of the Cosmos (ARCSEC) that is funded by the Korea Science and Engineering Foundation and the Ministry of Science and Technology.

REFERENCES

Adams, T. F., 1972, The Escape of Resonance Line Radiation from Extremely Opaque Media, ApJ, 174, 439

Ahn, S. -H., Lee, H. -W., & Lee, H. M., 2001, Ly α Line Formation in Starbursting Galaxies. I. Moderately Thick, Dustless, and Static H I Media, JKAS, 33, 29

Avrett, E. H. & Hummer, D. G., 1965, Non-coherent scattering, II: Line formation with a frequency independent source function, MNRAS, 130, 295

Bonilha, J. R. M., Ferch, R., Salpeter, E. E., & Slater, G., 1979, Monte Carlo calculations for resonance scattering with absorption or differential expansion, ApJ, 233, 649

Feibelman, W., 1983, Profiles and intensity ratios of the C IV lambda 1548, 1550 emission lines in planetary nebulae, A&A, 122, 335

Frisch, H., 1980, Scaling laws for resonance line photons in an absorbing medium, A&A, 87, 357

Harrington, J. P., 1973, The scattering of resonance-line radiation in the limit of large optical depth, MNRAS, 162, 43

Harries, T. J. & Howarth, I. D., 1996, Raman scattering in symbiotic stars. I. Spectropolarimetric observations, A&AS, 119, 61

Hummer, D. G., 1962, Non-coherent scattering: I. The redistribution function with Doppler broadening, MNRAS, 125, 21

Hummer, D. G. & Rybicki, G. B., 1971, The Formation of Spectral Lines, ARAA, 9, 237

Hummer, D. G. & Rybicki, G. B., 1982, A unified treatment of escape probabilities in static and moving media. I - Plane geometry, ApJ, 254, 767

Kafatos, M., Michalitsianos, A. G., & Fahey, R. P., 1985, High-dispersion ultraviolet spectra of the peculiar star RX Puppis, ApJS, 59, 785

Kenyon, S., 1986, The Symbiotic Stars, Cambridge University Press, New York

Laor, A., Bahcall, J. N., Jannuzi, B. T., Schneider, D. P., & Green, R. F., 1995, The Ultraviolet Emission Properties of 13 Quasars, ApJS, 99, 1

Lee, H. -W. & Kang, S., 2007, Raman-scattered O VI 6825 and the Accretion Disk Emission Model in the Symbiotic Stars V1016 Cygni and HM Sagittae, ApJ, 669, 1156

Lee, H. -W. & Park, M. -G., 1999, Toward the Evidence of the Accretion Disk Emission in the Symbiotic Star RR Telescopii, ApJ, 515, L89

Mastrodemos, N. & Morris, M., 1998, Bipolar Preplanetary Nebulae: Hydrodynamics of Dusty Winds in Binary Systems. I. Formation of Accretion Disks, ApJ, 497, 303

Michalitsianos, A. G., Kafatos, M., Fahey, R. P., Viotti, R., Cassatella, A., & Altamore, A., 1988, The C IV doublet ratio intensity effect in symbiotic stars., ApJ, 331, 477

Mikolajewska, J., Friedjung, M., & Quiroga, C., 2006, Line formation regions of the UV spectrum of CI Cygni, A&A, 460, 191

Mürset, U., Nussbaumer, H., Schmid, H. M., & Vogel, M., 1991, Temperature and luminosity of hot components in symbiotic stars, A&A, 248, 458,

Neufeld, D., 1990, The transfer of resonance-line radiation in static astrophysical media, ApJ, 350, 216

Osterbrock, D., 1989, Astrophysics of the Gaseous Nebulae and Active Galactic Nuclei, (University Science Books, Mill Valley)

Rybicki, G. B. & Lightman, A. P., 1979, Radiative Processes in Astrophysics, (Wiley-Interscience, New York)

Schmid, H. M., 1989, Identification of the emission bands at 6830, 7088 A, A&A, 211, L31

Schmid, H. M. et al., 1999, ORFEUS spectroscopy of the O VI lines in symbiotic stars and the Raman scattering process, A&A, 348, 950

Stenflo, J. O., 1980, Resonance-line polarization. V - Quantum-mechanical interference between states of different total angular momentum, A&A, 84, 68

Vetterling, W. T., Teukolsky, S. A., & Press, W. H., 1985, Numerical Recipes, Cambridge University Press, Cambridge

Yoo, J. J., Lee, H. -W., & Ahn, S. -H., 2002, Profiles of the resonance doublets formed in bipolar winds in symbiotic stars, MNRAS, 334, 974